

Spin-Orbit Scattering and Magnetoconductance of Strongly Localized Electrons

Ernesto Medina^(a) and Mehran Kardar

Department of Physics, Massachusetts Institute of Technology, Cambridge, Massachusetts 02139

(Received 21 February 1991)

The effect of a magnetic field on the tunneling probability of strongly localized electrons is calculated in the presence of spin-orbit scattering. Numerical (transfer matrix) and theoretical (replica analysis) arguments indicate a positive magnetoconductance, but no increase in the localization length. Universal and nonuniversal aspects of the tunneling probability distribution, and their relation to the symmetries of the Hamiltonian, are discussed.

PACS number(s): 71.55.Jv, 05.40.+j, 72.20.Dp, 75.10.Nr

The role of quantum interference effects on magnetoconductance (MC) and conductivity fluctuations has been extensively studied for *weakly localized* electrons.¹ In the absence of spin-orbit scattering (SO), a magnetic field causes an increase in the localization length (a positive MC), and a factor of 2 decrease in the conductance fluctuations. These results are attributed to suppression of *backscattering* loops by a magnetic field. With SO, the magnetic field has the opposite effect of decreasing the localization length (a negative MC), but still reduces the conductance fluctuations.² Symmetries of the underlying Hamiltonian, and their modification by a magnetic field, can also be invoked to support these conclusions.³

The behavior of conductivity and its fluctuations for *strongly localized* electrons is, however, more controversial and less well understood. The main mechanism for conductivity in this regime is by electron tunneling.⁴ Nguyen, Spivak, and Shklovskii⁵ (NSS) have emphasized that one must account for the quantum interference of *forward-scattering* paths to the tunneling probability. Treatments that ignore the correlations between such paths conclude a positive magnetoconductance, but no change in the localization length, whether in the absence^{5,6} or presence⁷ of SO. On the other hand, a random-matrix approach⁸ predicts that a magnetic field leads to a doubling of the localization length ξ (big, positive MC) without SO, but a halving of ξ (big, negative MC) in the presence of SO. Previously we demonstrated, within the NSS model,⁹ that without SO a magnetic field leads to a small increase in the localization length. Here we demonstrate that with SO, there is still a positive MC, but no change in the localization length. We also discuss why our results differ from those obtained by other approaches.

The starting point is the Anderson-type Hamiltonian

$$\mathcal{H} = \sum_{i,\sigma} \epsilon_i a_{i,\sigma}^\dagger a_{i,\sigma} + \sum_{\langle ij \rangle, \sigma\sigma'} V_{ij,\sigma\sigma'} a_{i,\sigma}^\dagger a_{j,\sigma'}, \quad (1)$$

where ϵ_i are the random-site energies. The nearest-neighbor-only hopping elements are set to $V_{ij} = VU_{ij}$, where V is a constant, and each U_{ij} is a randomly chosen SU(2) matrix, describing the spin rotation due to strong

SO on each bond.^{3,7} The tunneling probability between two sites is related to their overlap, which using a “locator” expansion¹⁰ can be written as

$$\langle i\sigma | G(E) | f\sigma' \rangle = \sum_{\Gamma} \prod_{i_r} \frac{V e^{i\mathcal{A}} U}{E - \epsilon_{i_r}}. \quad (2)$$

The above expression is a Feynman sum over all possible trajectories Γ between the initial (i) and final (f) sites, as derived by standard perturbation theory. Each bond along the path contributes a random spin rotation U , and a phase factor from the magnetic vector potential \mathcal{A} . To simplify the energy denominators, we use the NSS model⁵ in which the energy of the initial and final sites is set to zero, while the intermediate ϵ_i take on values of $+\epsilon$ or $-\epsilon$ with equal probability. A path of length l now contributes an amplitude $\epsilon(V/\epsilon)^l$ to the sum, as well as an overall sign and rotation matrix. In the localized regime, the sum is rapidly convergent, dominated by its first few terms.¹⁰ [Clearly the sum is bounded by one in which all terms make a *positive* contribution, i.e., by a lattice random walk, which is convergent for $z(V/\epsilon) < 1$, where z is the lattice coordination number. This provides a lower bound for the delocalization transition.] Thus for $V/\epsilon \ll 1$, corresponding to strongly localized electrons, Eq. (2) is dominated by the shortest paths connecting the end points. Following NSS, we maximize the interference between such *forward-scattering* paths by choosing i and f to lie along the diagonal of a square lattice, as in Fig. 1. All shortest paths Γ' now have the same length t , and the tunneling amplitude simplifies to

$$A = \langle i\sigma | G(0) | f\sigma' \rangle = \epsilon(V/\epsilon)^t J(t), \quad (3)$$

$$J(t) = \sum_{\Gamma'} \prod_{i_r} \text{sgn}(\epsilon_{i_r}) e^{i\mathcal{A}} U.$$

After averaging over the initial spin, and summing over the final spin, the tunneling probability is

$$T = \frac{1}{2} \text{Tr}(A^\dagger A) = \epsilon^2 (V/\epsilon)^{2t} I(t), \quad (4)$$

$$I(t) = \frac{1}{2} \text{Tr}(J^\dagger J).$$

The overlap is expected to typically decay as $\exp(-t/\xi)$,

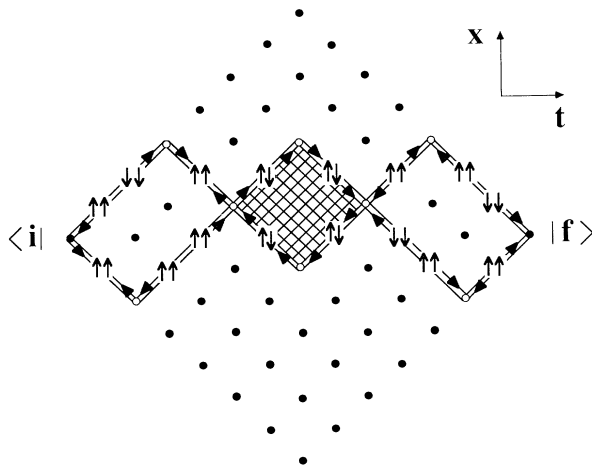


FIG. 1. Directed paths contributing to the tunneling between diagonally separated end points. The averaging over SO pairs forward and time-reversed paths, and their spins, as indicated.

where ξ is the localization length. From Eqs. (3) and (4) we see that $\xi^{-1} = \xi_0^{-1} + \xi_g^{-1}$, i.e., the localization length has a *local* contribution $\xi_0^{-1} = \ln(\epsilon/V)$, and a *global* contribution $\xi_g^{-1} = -\ln I(t)/2t$. The latter contains all the important quantum interference information.

We numerically studied the statistical properties of $I(t)$, using a transfer-matrix method to exactly calculate I up to $t = 1000$, for over 2000 realizations of the random Hamiltonian. As before⁹ we found that the distribution is broad (almost log-normal), and that the appropriate variable to consider is $\ln I(t)$. In Fig. 2 we have plotted $\langle \ln I(t) \rangle$ vs t , with and without SO and at various magnetic fields. In all cases, the asymptotic slope gives the global contribution ξ_g^{-1} to the (inverse) localization length. We first note that the introduction of SO is accompanied by a significant increase in tunneling, i.e., an increase in ξ . Second, the addition of a magnetic field leads to an increase in $\langle \ln I(t) \rangle$, but in qualitatively different manners in the absence or presence of SO. Without SO, there is a change in slope, i.e., the most important effect of the field is to increase the localization length. This is an enhancement of tunneling that grows exponentially in t . By contrast, with SO, we observe that the slopes in Fig. 2 remain unchanged. Thus the effect of the magnetic field is to enhance the tunneling rate by a t -independent constant, i.e., there is no change in the localization length. Finally, Fig. 3 indicates that we can collapse the data for different values of B and t , using the combination $Bt^{3/2}$ as the argument. In fact, the behavior of the scaling function is

$$\langle \ln I_{SO}(t, B) \rangle - \langle \ln I_{SO}(t, 0) \rangle = \begin{cases} cB^2 t^3 & \text{if } B^2 t^3 < 1, \\ C & \text{if } B^2 t^3 > 1. \end{cases} \quad (5)$$

We can gain some analytic understanding of the dis-

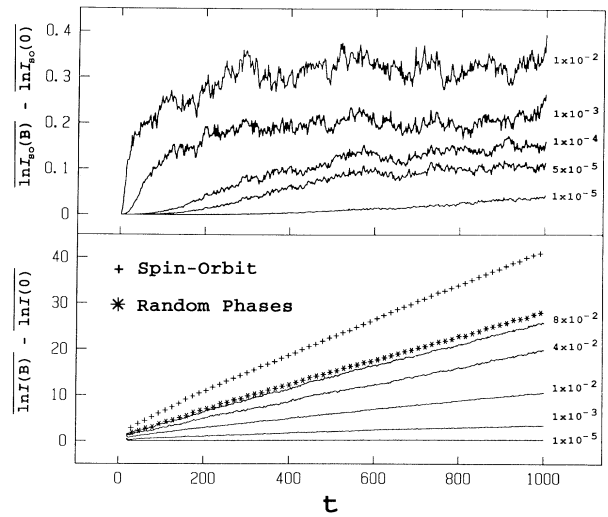


FIG. 2. Log-averaged tunneling probability vs t , with and without SO, and at various magnetic fields shown on the right. Bottom: Increase in tunneling (MC) (solid lines), *without SO*, from the zero-field value $I(0)$. Saturated behavior in a strong magnetic field (asterisks) is simulated by replacing the gauge potential with random phases on bonds. Addition of SO in zero field leads to the curve with plusses. Top: Since MC *with* SO is small, the increase is plotted at enlarged scale.

tribution function for $I(t, B)$ by examining the moments $\langle I(t)^n \rangle$. From Eqs. (3) and (4) we see that each $I(t)$ represents a forward path from i to f , and a time-reversed path from f to i . For $\langle I(t)^n \rangle$, we have to average over the contributions of n such pairs of paths. First, averaging over the random signs of the site energies forces a pairing of the $2n$ paths (since any site crossed by an odd number of paths leads to a zero contribution).⁹ Next we must average over the random SO matrices on

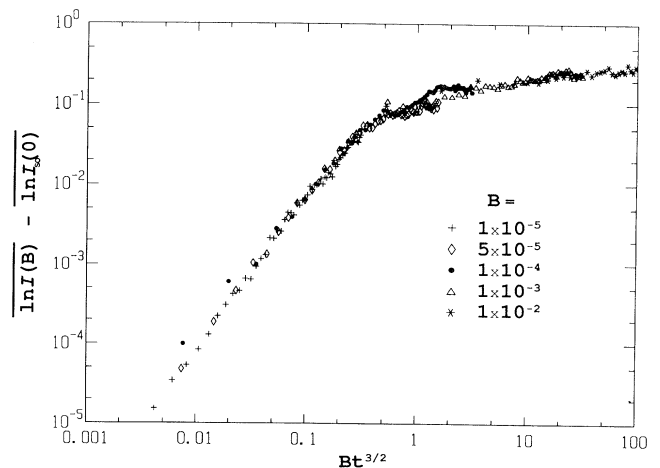


FIG. 3. Scaling of MC in the presence of SO from the top part of Fig. 2 with B and t .

each bond. Again a bond crossed only once gives zero average ($\langle U_{\alpha\beta} \rangle = 0$). From the orthogonality theorem of group representations it can be shown that only the following paired averages are nonzero:

$$\langle U_{\alpha\beta} U_{\alpha\beta}^* \rangle = \frac{1}{2}, \quad \langle U_{\uparrow\uparrow} U_{\uparrow\uparrow} \rangle = \frac{1}{2}, \quad \langle U_{\uparrow\downarrow} U_{\uparrow\downarrow} \rangle = -\frac{1}{2}, \quad (6)$$

and their complex conjugates. Thus two classes of paired paths survive the averaging: (1) *Neutral paths* in which one member is selected from J and the other from J^\dagger . Such paths are forced to have parallel spins and do not couple to the magnetic field. (2) *Charged paths* in which both elements are taken from J or from J^\dagger . Such pairs must have antiparallel spins and couple to the magnetic field like particles of charge $\pm 2e$. These constraints are indicated in Fig. 1 which shows a possible contribution to $\langle I^2 \rangle$.

Since at each site any path has a choice of two directions, we may naively expect $\langle I(t)^n \rangle$ to asymptotically scale as 2^n . [The factor of $\frac{1}{2}$ from the bond averages in Eq. (6) cancels with the choice of two spin directions at each site.] This ignores the correlations between paths which manifest themselves when two paired paths intersect.¹¹ Since at each intersection the pairs may exchange partners there is an additional statistical attraction for such crossings. The attraction factor is⁹ 3 with $B=0$ and no SO (orthogonal symmetry), and decreases to 2 in strong fields (unitary symmetry). With SO, we must also take into account the allowed spin exchanges, and we find that the intersection of two paired paths results in an exchange attraction of $\frac{3}{2}$ (symplectic symmetry). The sum over n attracting paths then leads to⁹

$$\langle I(t)^n \rangle = A(n) 2^n \exp[\rho n(n^2 - 1)t]. \quad (7)$$

The effect of correlations is thus described by the parameter ρ , which is an increasing function of the strength of the attraction between paths. We have also included an overall amplitude $A(n)$. From the scaling of the moments with n , it follows that $\ln I(t)$ is approximately normal, with mean and fluctuations given by

$$\langle \ln I(t) \rangle = (\ln 2 - \rho)t, \quad \text{var}[\ln I(t)] \sim (\rho t)^{2/3}. \quad (8)$$

[We have numerically confirmed the $\frac{2}{3}$ power law for the variance of $\ln I(t)$ with and without SO.]

We can now appreciate the trends in Fig. 2, as the slopes are indicative of the statistical attraction factors. Without SO, the magnetic field gradually reduces the attraction factor from 3 to 2 leading to the increase in slope. The addition of SO to the Hamiltonian has the similar effect of suddenly decreasing the attraction to $\frac{3}{2}$. Why does the addition of the magnetic field lead to no further change in ρ in the presence of SO? Without SO the origin of the continuous change in the attraction factor is the type of exchange indicated in Fig. 1, whereby a charged bubble appears from the intersection of two neutral paths.⁹ In the presence of SO, from the averages in Eq. (6) we calculated the contribution of such configura-

tions to be zero. Thus the neutral paths traverse the system without being affected by the magnetic field; their attraction factor, and hence ρ and ξ , remain unchanged. The smaller positive MC observed in the simulations is due to the quenching of the charged paths by a magnetic field. The resulting change is thus only in the amplitude $A(n)$ of Eq. (7). Certainly the above discussion is too terse and conveys only the essence of the arguments. We defer a more detailed discussion to future publications so that in the remaining space we can summarize the implications of our results, and contrast them with related works.

(1) A one-parameter scaling assumption¹² is the cornerstone of the scaling approach to weak localization,¹ and has also been extended to the localized regime.^{8,13} From Eqs. (4) and (7) we see that description of the tunneling probability requires at least two parameters, as the localization length ξ depends on the *local* factor ϵ/V , as well as the *global* factor ρ . However, ρ does control the nontrivial scaling of the distribution (up to the amplitude A). We further note that Eq. (7) is only valid for low moments, i.e., near the peak of the distribution for $\ln I$. The behavior of very high moments, i.e., the tail of the distribution, is found to be nonuniversal and reflects the local behavior of the random potential. Similar nonuniversal scaling of moments has been reported recently close to the localization transition.¹⁴ To make a concrete connection between the two limits, we need, however, a better understanding of the relation between the tunneling probability in Eq. (4) and the dimensionless conductivity g studied in the scaling approach.¹

(2) In the independent-path approximation (IPA),^{5,6} correlations leading to the nontrivial scaling of moments in Eq. (7) are ignored. Hence $\langle I^n \rangle = A(n) 2^n$, and the MC reflects the changes in the amplitude $A(n)$. Without SO, all pairings of $2n$ paths contribute equally at $B=0$ [$A(n, B=0) = (2n-1)!!$], while only neutral paths survive at finite field [$A(n, B \neq 0) = n!$]. The difference between these two numbers at $n=0$ gives the increase by $\ln 2$ of $\langle \ln I \rangle$ predicted by IPA.⁶ Recent experiments at low temperatures¹⁵ observe increases in relative conductance by factors much larger than unity, in disagreement with IPA, but consistent with Fig. 2. Although IPA clearly fails without SO, it is close to the mark in the presence of SO as the observed initial increase of $B^2 t^3$ [Eq. (5)] precisely follows from the quenching of charged paths. Using the IPA, Meir *et al.*⁷ predict a universal increase of $C = \frac{5}{6} - \ln 2 \approx 0.140$ in $\ln I$ for sufficiently strong fields [see Eq. (5)]. Our numerical results yield a saturation value of $C \approx 0.32$. However, we believe this increase is nonuniversal, as the behavior changed once we reduced the concentration of SO impurities.

(3) The random-matrix approach (RMA) to the problem^{3,8,13} takes as its input only the symmetries of the Hamiltonian, and the assumption of a single-parameter scaling. It predicts⁸ that the magnetic field results in

doubling of the localization length ξ in the absence of SO, and a halving of ξ with SO, in clear contradiction to our results. Despite its simplicity and generality, RMA has a number of shortcomings. First, it is assumed at the outset that a single parameter is sufficient for characterizing the problem. As we demonstrated, description of the localization length (using the tunneling probability) requires both a global and a local factor; hence variations in ξ cannot be universal. Second, by considering the most general random matrices the approach loses all information on spacial connectivity and dimensionality. (The equivalent approximation for spin problems allows any spin in one layer to interact with *all* spins in neighboring layers. Thus it has the flavors of both one-dimensional and infinite-range models.) The correct approach is to consider the ensemble of sparse random matrices in which only elements close to the diagonal are nonzero. Finally, symmetry arguments imply that the addition of a magnetic field, by destroying time-reversal symmetry, immediately changes a system with or without SO to one completely described by a unitary ensemble. In fact, from Fig. 2, we do see that the magnetic field in the absence of SO derives the localization length towards its unitary limit (obtained by placing random phases on each bond). However, the change in ξ is gradual, and not immediate. Furthermore, there is no change in ξ with SO. The latter is due to the form of the Hamiltonian. To reach the unitary limit with SO, one has to also include Zeeman-splitting terms. Such terms are certainly allowed by symmetry, but involve a much higher energy cost. RMA cannot account for such subtleties.

(4) Recent experiments on Au-doped In_2O_3-x films¹⁶ observe a transition from negative MC at small disorder to positive MC at large disorder. This is attributed¹⁶ to an interplay between weak-localization effects (causing negative MC with SO) at scales less than ξ , and strong-localization effects (positive MC) at scales larger than ξ . To account for the insensitivity to the addition of Au, it is also suggested¹⁶ that addition of SO has little effect on the strongly localized regime. This is in conflict with the results of Fig. 2 at high concentrations of SO. However, a more dilute SO concentration may not be in contradiction with the experimental results. We also note that the sign of MC at small fields cannot be changed by what goes on at short distances. The local contribution to $\langle \ln T \rangle$ in Eq. (4) must be analytic, and scale as $B^2 t$, while the global change in $\langle \ln T \rangle$ scales as $B^2 t^3$ [Eq. (5)]. Hence there is always a positive MC at low fields at sufficiently large t (it may cross over to a negative MC at

higher fields). Numerical simulations⁷ at the scale of ξ are in agreement with such a picture. If a positive MC is a signature of the localized regime, it can only be reconciled with a negative MC predicted by the weak-localization theories with strong SO through a possible phase transition.¹⁷ Could the observed change of sign in the experiments be a finite-temperature manifestation of such a zero-temperature phase transition?⁷ Certainly more experimental and theoretical studies are in order.

We have benefited from discussions with B. Altshuler, Y. Meir, Y. Shapir, and N. Wingreen. This research was supported by the NSF through Grant No. DMR-90-01519, the Presidential Young Investigator program.

^(a)Permanent address: Intevep S.A., Apartado Postal 76343, Caracas 1070A, Venezuela.

¹For recent reviews, see P. A. Lee and T. B. Ramakrishnan, *Rev. Mod. Phys.* **57**, 287 (1985); G. Bergmann, *Phys. Rep.* **107**, 1 (1984).

²B. L. Altshuler and B. I. Shklovskii, *Zh. Eksp. Teor. Fiz.* **91**, 220 (1986) [*Sov. Phys. JETP* **64**, 127 (1986)]; P. A. Lee, A. D. Stone, and H. Fukuyama, *Phys. Rev. B* **35**, 1039 (1987); F. J. Wegner, *Z. Phys. B* **35**, 207 (1979).

³N. Zannon and J. L. Pichard, *J. Phys. (Paris)* **49**, 907 (1988).

⁴O. Faran and Z. Ovadyahu, *Phys. Rev. B* **38**, 5457 (1988).

⁵V. L. Nguyen, B. Z. Spivak, and B. I. Shklovskii, *Pis'ma Zh. Eksp. Teor. Fiz.* **41**, 35 (1985) [*JETP Lett* **41**, 42 (1985)]; *Zh. Eksp. Teor. Fiz.* **89**, 11 (1985) [*Sov. Phys. JETP* **62**, 1021 (1985)].

⁶O. Entin-Wohlman, Y. Imry, and U. Sivan, *Phys. Rev. B* **40**, 8342 (1989).

⁷Y. Meir, N. S. Wingreen, O. Entin-Wohlman, and B. L. Altshuler, *Phys. Rev. Lett.* **66**, 1517 (1991).

⁸J. L. Pichard, M. Sanquer, K. Slevin, and P. Debray, *Phys. Rev. Lett.* **65**, 1812 (1990).

⁹E. Medina, M. Kardar, Y. Shapir, and X. R. Wang, *Phys. Rev. Lett.* **62**, 941 (1989); **64**, 1816 (1990).

¹⁰P. W. Anderson, *Phys. Rev.* **109**, 1492 (1958).

¹¹Y. Shapir and X. R. Wang, *Europhys. Lett.* **4**, 1165 (1987).

¹²E. Abrahams, P. W. Anderson, D. C. Licciardello, and T. V. Ramakrishnan, *Phys. Rev. Lett.* **42**, 673 (1979).

¹³K. A. Muttalib, *Phys. Rev. Lett.* **65**, 745 (1990).

¹⁴B. L. Altshuler, V. E. Kravstov, and I. V. Lerner, *Phys. Lett. A* **134**, 488 (1989); see, however, B. Shapiro, *Phys. Rev. Lett.* **65**, 1510 (1990).

¹⁵F. P. Milliken and Z. Ovadyahu, *Phys. Rev. Lett.* **65**, 911 (1990).

¹⁶Y. Shapir and Z. Ovadyahu, *Phys. Rev. B* **40**, 12441 (1989).

¹⁷N. Evangelou and T. Ziman, *J. Phys. C* **20**, L235 (1987).